

Benefits of assimilating SAPHIR observations on analysis and forecasts of tropical fields in the Met Office global model

A. Doherty¹ | S. Indira Rani² | S. Newman¹ | W. Bell³

¹Satellite Applications, Met Office, Exeter, UK

²National Centre for Medium Range Weather Forecasting (NCMRWF), Noida, India

³Reanalysis Group, Copernicus Climate Change Service, ECMWF, Reading, UK

Correspondence

A. Doherty, Met Office, FitzRoy Road, Exeter, Devon EX1 3PB, UK.

Email: amy.doherty@metoffice.gov.uk

Funding information

NWPSAF Visiting Scientist Program. Ministry of Earth Sciences, Government of India. Indian National Monsoon Mission.

The Sondeur Atmosphérique du Profil d'Humidité Intertropicale par Radiométrie (SAPHIR) instrument provides improved sampling of tropical atmospheric moisture vertically, horizontally and temporally. The impact of these unique characteristics is investigated through: an idealised study of retrieved humidity profiles; single-observation experiments; assimilation experiments in a global NWP system; and an investigation into the spin-down of precipitation in the early phase of the forecast. SAPHIR offers improved performance over similar satellite instruments, and beneficial impacts were found in all investigations. When assimilated in conjunction with observations from the Advanced Microwave Scanning Radiometer imager AMSR-2 the impact is further improved. Retrieval studies showed the errors in retrievals from SAPHIR were lower than those obtained from MHS or ATMS at all levels above 600 hPa. Single-observation experiments showed that, when assimilated together with AMSR-2, AMSR-2-driven humidity increments were modified to give more realistic vertical structure. In assimilation experiments employing a near-operational configuration of the Met Office global model, the assimilation of clear-sky SAPHIR data improved the root-mean-square errors of a number of forecast metrics, most notably temperature at 250 hPa (improved by 2%), relative humidity at 500 hPa (2%) and wind at 500 hPa (1%) at forecast lead times of 12 and 24 h. The results of this work form a clear recommendation for future remote-sensing missions including both SAPHIR and AMSR-2 channel configurations.

KEYWORDS

AMSR-2, assimilation, atmospheric moisture, Megha-Tropiques, microwave imaging, microwave sounding, NWP, SAPHIR

1 | INTRODUCTION

The Sondeur Atmosphérique du Profil d'Humidité Intertropicale par Radiométrie (SAPHIR) is a microwave humidity sounder carried on board the Megha-Tropiques (MT) satellite. MT is a joint Indo-French satellite mission launched in October 2011 to study the tropical water budget (Vijayasree *et al.*, 2014; Roca *et al.*, 2015). The low inclination orbit allows more frequent observations of the tropical belt (between latitudes of $\pm 30^\circ$) relative to polar orbiting satellites. In addition to SAPHIR it carries three other instruments: a microwave imager Microwave Analysis and Detection of Rain and

Atmospheric Structure (MADRAS); Scanner for Radiation Budget (ScaRaB), a broad-band radiometer for monitoring the Earth's radiation budget; and ROSA, a radio occultation sounder. The microwave imager, MADRAS, has channels at 18, 23, 36, 89 and 157 GHz and was intended to complement SAPHIR by providing cloud detection and surface information. It was deactivated in September 2013 after a deterioration in performance from January 2013.

Due to the paucity of *in situ* water vapour measurements in the Tropics and the relatively poor vertical resolution and coverage of other satellite-borne humidity sounders, there exists an ongoing requirement for improved observations of

TABLE 1 Channel frequencies of all existing satellite radiometer channels around the 183 GHz water vapour line

Instrument	Channel number										
chan freq offset from 183.31 GHz	± 0.2	± 1.0	± 1.1	± 1.8	± 2.7	± 3	± 4.2	± 4.5	± 6.6	± 7.0	± 11.0
AMSU-B/MHS		3				4				5	
SSMIS		11				10			9		
MWHS1		3				4				5	
ATMS		22		21		20		19		18	
MWHS2		11		12		13		14		15	
GPM-GMI						12				13	
SAPHIR	1	2	3			4			5	6	

tropical moisture. By providing higher vertical resolution measurements with more frequent revisits, SAPHIR has been designed to improve the sampling of the diurnal cycle of water vapour and the evolution of convective systems.

SAPHIR is a six-channel cross-track scanning microwave sounding radiometer with a maximum scan angle of 43°. It has 130 resampled fields of view per swath at a (nadir) resolution of 10 km (Vijayasree *et al.*, 2014). The six SAPHIR channels are centred at 183 GHz, in the wings of the water vapour line. They provide weighting functions with contributions from the surface to \sim 12 km which peak, depending on water vapour burden, between the top of the boundary layer and 10 km. These provide better vertical resolution and coverage for humidity sounding than other similar instruments and are therefore expected to deliver benefits over these (Brogniez *et al.*, 2013). For example the Microwave Humidity Sounder (MHS) and the Advanced Microwave Sounding Unit-B (AMSU-B) on board the National Oceanic and Atmospheric Administration (NOAA) and MetOp polar orbiting satellites have three channels around the 183 GHz line, while the Advanced Technology Microwave Sounder (ATMS) flown on Suomi National Polar-orbiting Partnership (SNPP) satellite has five. Table 1 shows the channel frequencies of existing satellite-borne humidity sounders around the 183 GHz water vapour line. SAPHIR also extends vertical coverage, relative to MHS/ATMS, both closer to the surface with the 183 ± 11.0 GHz channel which typically peaks below 600 hPa, and higher in the atmosphere with the 183 ± 0.2 GHz channel, which typically peaks around 300 hPa. Figure 1 compares typical tropical weighting functions for MHS, SAPHIR and ATMS channels calculated using the Radiative Transfer for TIROS Operational Vertical sounder (RTTOV9) fast radiative transfer model (Saunders, 2010); the temperature and specific humidity profiles are also shown, as the weighting function shape is dependent on these. A more humid atmosphere narrows the weighting function and pushes the peak higher in the atmosphere. The 183 ± 11.0 GHz channel offers a significant advantage over the window channels of MHS at 89 and 157 GHz, for example, insofar as it acts as a “clean” sounding channel in the Tropics, exhibiting minimal sensitivity to surface effects which are prone to errors in emissivity and skin temperature.

In addition, SAPHIR is unique in the temporal frequency of its observations as the 20° inclination of the MT orbit allows high temporal sampling in the tropical belt of 2–5 times a day for a given point.

A number of studies have been carried out to evaluate the quality of the SAPHIR data. Singh *et al.* (2013) compared SAPHIR observations with simulated radiances, using a radiative transfer model (RTM), taking both radiosonde profiles and profiles retrieved from AIRS data as input. They also compared SAPHIR and MHS brightness temperatures and found good agreement with biases (standard deviations) for SAPHIR channels 1–6 of 3.74 (2.45), 1.83 (2.22), 0.10 (1.79), -0.64 (1.62), -0.83 (1.56), and -1.64 (1.54) K, respectively. Their study shows the impact of SAPHIR radiances on the Weather Research and Forecasting (WRF) 3D-Var data assimilation system, with errors reduced by up to 17% in the tropospheric analyses and forecasts of moisture, temperature, winds and precipitation.

Chambon *et al.* (2015) investigated the impact of SAPHIR radiances in the global numerical weather prediction (NWP) model operational at Météo-France, Action des Recherche Petit Echelle et Grand Echelle (ARPÈGE); they found that the combination of the MT low inclination orbit with SAPHIR’s six channels increased the number of assimilated humidity-sensitive microwave observations in the Tropics by a factor of 3.8, compared to the control experiment in which three AMSU-B/MHS microwave sounders were assimilated. Chambon *et al.* (2015) demonstrated benefit in assimilating SAPHIR data both on analyses and on forecasts, with relative humidity RMSE reduced by \sim 10% between 400 and 150 hPa for 12 h forecasts.

Clain *et al.* (2015) compared the SAPHIR brightness temperature observations with those simulated by an RTM using *in situ* radiosonde observations as input and found that the mean bias agrees with that found by other studies for other instruments (e.g. Moradi, 2014). They also discussed the fact that the magnitude of the bias depends on the channel, increasing from 0.18 K for the 183 ± 0.2 GHz channel to 2.3 K for the 183 ± 11.0 GHz channel; this pattern of systematic bias was also seen in other studies, including the works summarised here. The reason for this variation in bias with frequency is not fully understood, though it is observed in

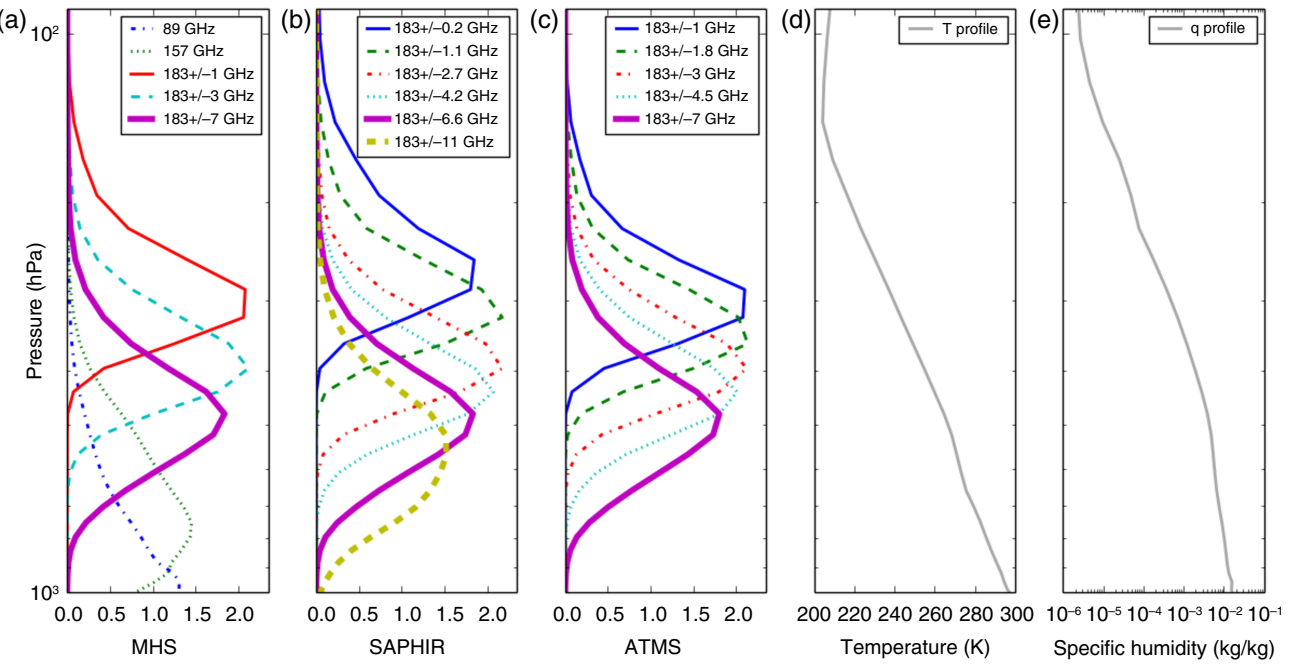


FIGURE 1 Examples of weighting functions for (a) MHS, (b) SAPHIR, and (c) ATMS for a tropical atmospheric profile at 29°N, 71°W on 1 July 1993 at 0000 UTC from the Chevalier (2015) dataset, showing the increased vertical coverage provided by SAPHIR over the other instruments. (d) and (e) show, respectively, the temperature and specific humidity profile for the point used [Colour figure can be viewed at wileyonlinelibrary.com]

all satellite-borne instruments with channels around 183 GHz and it is likely that it arises from a combination of distinct sources. Further discussion can be found in Brogniez *et al.* (2016), but is outside the scope of this work. Bias-corrected observations are used in the experiments presented here, so this pattern of biases does not affect results.

This article explores the use of SAPHIR as utilised within the Met Office operational system. Section 2 presents the operational set-up for SAPHIR and the other instruments, highlighting the theoretical and empirical evidence which led to the different treatment of the 183 GHz channels on ATMS, MHS and SAPHIR. The differences in observation error are the result of operational tuning at the point of use, to maximise the benefit of assimilating each particular data type, and further explanation is given in this section.

The particular benefits associated with the enhanced channel set of SAPHIR are then investigated through an idealised one-dimensional variational (1D-Var) retrieval study (Smith, 2016) which is described in section 3. Related to this, section 4 presents a number of single-observation experiments performed within the more realistic assimilation framework of the Met Office's incremental 4D-Var system, and examines how SAPHIR observations modify analysis increments. Section 5 outlines the results of assimilating SAPHIR observations in the Met Office global NWP system. Section 6 explores the effect of assimilating SAPHIR observations on the spin-down of precipitation through the early phase of the Met Office forecast, which indicates the extent to which the resulting moisture analysis is in balance with the representation of moist processes in the nonlinear forecast model. Conclusions are presented in section 7.

2 | INSTRUMENT CONFIGURATION

The pre-processing, quality control and observation errors for each instrument in this study are those used operationally at the Met Office. These are based on various factors such as data source, requirement for remapping, instrument artefacts and sometimes practical considerations required to obtain benefit from the instrument in Operations. The exception to this is for the 1D-Var experiments (section 3) where operational configuration was not required.

This section explains the differences in the operational treatment of SAPHIR and the 183 GHz channels on the other instruments (MHS channels 3–5 and ATMS channels 18–22). The observation errors are shown in Table 2. The value from the diagonal R-matrix (observation plus forward model error covariance matrix) from Met Office operations is given, with the pre-launch value of NEAT from the Observing Systems Capability Analysis and Review (OSCAR) database quoted next to it in brackets (World Meteorological Organisation, 2017). MHS and ATMS 183 GHz channel operational observation errors are higher than those used for SAPHIR due to empirical tuning at operational implementation. The reasons why such different values were necessary to deliver benefit from essentially similar channel sets can be attributed to the pre-processing and quality control of each instrument type, summarised for both operational experiments (sections 5 and 6) and 1D-Var experiments (section 3) in Table 3. The tuning of observation errors is standard practice at the Met Office and is the reason why AMSR-2 observation errors are also higher than NEAT values, as these were increased before operational use to account for deficiencies in the liquid-water path (LWP) check for this instrument.

TABLE 2 Observation errors (K) for each instrument channel. The first value is from the R-matrix used operationally within the Met Office system and used for all experiments in this article except the 1D-Var. The value in the brackets is the NE Δ T for the instrument and was used as the error added to the synthetic noise-free brightness-temperature simulations before running 1D-Var and the observation error within the 1D-Var in section 3, the shading in the table is simply to allow easier identification of which channels belong to which instrument

Instrument Channel frequency (GHz)	MHS	ATMS	AMSR	SAPHIR
18.7 (H)			9.6 (0.6)	
18.7 (V)			5.6 (0.6)	
23.7 (H)			14.4 (0.6)	
23.7 (V)			7.6 (0.6)	
36.5 (H)			12.0 (0.6)	
36.5 (V)			5.6 (0.6)	
183 ± 0.2				1.5 (2.0)
183 ± 1.0	4.0 (0.57)	4.5 (0.9)		
183 ± 1.1			1.5 (1.5)	
183 ± 1.8		4.0 (0.8)		
183 ± 2.7			1.5 (1.5)	
183 ± 3.0	4.0 (0.42)	4.0 (0.8)		
183 ± 4.2			1.5 (1.3)	
183 ± 4.5		4.0 (0.8)		
183 ± 6.6			1.5 (1.3)	
183 ± 7.0		4.0 (0.8)		
190.311	4.0 (0.45)			1.5 (1.0)
183 ± 11.0				

Raw ATMS data are highly oversampled with associated high radiometric noise. For use in the Met Office operational system, ATMS is remapped by the Advanced TIROS Operational Vertical Sounder (ATOVS) and Advanced Very High Resolution Radiometer (AVHRR) Pre-processing Package (AAPP) (Numerical Weather Prediction Satellite Application Facility, 2011) to 40 km nadir resolution (3.3° beam width), reducing the noise by a factor of 0.23 to between 0.2 and 0.4 K (Doherty *et al.*, 2015), while SAPHIR is used at its native resolution of 10 km with an NE Δ T of 1–2 K.

In an initial study on the use of SAPHIR at the Met Office, R-matrix values for SAPHIR which matched those of ATMS 183 GHz channels (4 K for all channels) have been tested (Rani *et al.*, 2016). In this study the impact of SAPHIR is lower, as would be expected, but the conclusions agree with those found in section 5, namely that assimilating SAPHIR together with microwave imager observations adds value not seen when either instrument is assimilated alone.

As well as the differences in observation error and pre-processing, the quality control differs between the instruments.

SAPHIR is assimilated over all surfaces in clear conditions, with only a threshold check on the difference between observed and background brightness temperature of 20 K used to reject all channels. This check will reject the majority

of cases where high land impinges on the lower-peaking weighting functions or where ice cloud contaminates the field of view; it is similar in theory to the check on SAPHIR channel 6 used in Chambon *et al.* (2015), though their threshold is set at 5 K. It should be noted that, at the time of writing, a threshold of 10 K for the SAPHIR check and updated channel selection over different surfaces is being tested at the Met Office. In addition it can be noted the failed MADRAS instrument would have provided imaging channels for use in cloud detection for SAPHIR.

ATMS observations are assimilated over sea only and have stricter quality-control tests, utilising the lower-frequency temperature sounding channels. These comprise: a surface mismatch test from the AAPP (Labrot *et al.*, 2006) and the Bennartz rain test (Bennartz *et al.*, 2002), both of which reject all 183 GHz channels when triggered; a liquid water test using 23.31 and 50 GHz which rejects channel 18, the lowest-peaking channel; and a cirrus cost test which calculates a cost function from the 183 ± 1.0 , 3.0 and 7.0 GHz channels and rejects the three lowest-peaking channels (18–20) if it is over a threshold (Doherty *et al.*, 2012). These differences in pre-processing and observation error settings will influence the impact each instrument has on operational analyses. ATMS, with its higher observation errors, will have a smaller impact than SAPHIR. However, as these are the values used operationally at the Met Office, and this article assesses the effects of the instruments on the Met Office system, the results must necessarily be presented in this manner.

3 | 1D-VAR EXPERIMENTS

Idealised 1D-Var experiments were conducted to investigate whether SAPHIR observations provide a more accurate estimate of the atmospheric moisture profile than other microwave instruments (ATMS, MHS and AMSR-2) as suggested by the qualitative comparison of weighting functions shown in Figure 1. Five experiments were run using a 1D-Var to perform retrievals based on synthetic observations, with RTTOV12 used as the observation operator (Smith, 2016; Saunders *et al.*, 2017). A set of synthetic brightness-temperature observations were generated from 1,333 70-level tropical input profiles (Smith, 2016) which acted as a proxy for the true state of the atmosphere (or “truth”). These noise-free simulated brightness temperatures were then degraded through the addition of uncorrelated random noise to give “background” profiles. Noise values, expressed as noise-equivalent delta brightness temperatures (NE Δ Ts) were obtained from the WMO OSCAR database (World Meteorological Organisation, 2017) and are listed in brackets in Table 2; these values were also used for the observation error.

Background atmospheric profiles which serve as the *prior* atmospheric state in the 1D-Var and corresponding to T + 6 h forecasts, were generated through the addition of random

TABLE 3 Set-up for operational and 1D-Var experiments for each instrument

	SAPHIR	ATMS	MHS	AMSR-2
Preprocessing				
Footprint size (ssp)	10 km	16 km	16 km	10 km
Remapping	None	40 km	40 km	None
Resampling	None	1 spot in 3	None	None
1D-Var set-up				
RT calculations	Clear sky	Clear sky	Clear sky	Clear sky
Radiative transfer model	RTTOV 12	RTTOV 12	RTTOV 12	RTTOV 12
Ocean emissivity model	FASTEM-6	FASTEM-6	FASTEM-6	FASTEM-6
Surface type	Ocean surface only	Ocean surface only	Ocean	Ocean
Channels used	1–6	18–22	3–5	7–12
Observation errors	NEΔT	NEΔT	NEΔT	NEΔT
Operational set-up				
RT calculations	Clear sky	Clear sky	Clear sky	Clear sky
Radiative transfer model	RTTOV 9	RTTOV 9	RTTOV 9	RTTOV 9
Ocean emissivity model	FASTEM-2	FASTEM-2	FASTEM-2	FASTEM-2
Model horizontal resln	0.6°lon × 0.4°lat	0.6°lon × 0.4°lat	~25 km	~25 km
Channels used	1–6	6–15, 18–22	3–5	7–12
Thinning	One ob per 80 km/1 h	One ob per 80 km/1 hr	One ob per 80 km/1 h	One ob per 50 km/1 h
Operational Screening				
Land cover screening	All surfaces	Ocean only	Ocean only	Ocean only
Cloud screening	None	Scattering index/Bennartz/liquid water check/cirrus cost check	Same as ATMS	1D-Var LWP threshold
Additional screening	O–B < 20 K	O–B < 20 K	O–B < 20 K	O–B < 20 K

perturbations which were, by construction, consistent with the specified background error covariance matrix. The background error covariance was generated using a randomisation method which sampled errors from the full Met Office 4D-Var assimilation system (Fisher and Courtier, 1995).

Experiments were run for SAPHIR, AMSR-2, MHS and ATMS alone and then for a “super instrument” whose channel set is that of AMSR-2 and SAPHIR combined.

RTTOV12.1 was used to simulate the true and background brightness temperature for the super instrument, AMSR-2, ATMS, MHS and SAPHIR. The 1D-Var was then used to estimate the atmospheric state, given the synthesised observations, the accompanying background profile, and the error covariances associated with both. The true and retrieved profiles were then compared and the mean and standard deviation of the difference calculated. The exact settings used in the 1D-Var calculation are given in Table 3.

Figure 2 shows the standard deviation in the difference between retrieved and true profiles of specific humidity for each instrument averaged over the 1,333 tropical profiles, plotted directly (a), and as a percentage reduction relative to the background standard deviation (b).

Considering first the humidity sounders: ATMS, MHS and SAPHIR perform similarly; SAPHIR notably outperforms the other instruments between 650 and 900 hPa. This is likely to be a combination of the increased vertical

resolution and range throughout the atmosphere and the smaller observation errors, although the improvement at lower altitudes (800–900 hPa) due to the 183 ± 11.0 GHz channel is not as pronounced as might be expected, possibly because only tropical profiles have been selected in the 1,333 set, which are likely to have a higher water vapour burden, pushing the peak of SAPHIR channel 6 higher in the atmosphere.

Secondly consider the performance of AMSR-2 and SAPHIR and their combined impact in the super instrument. AMSR-2 has the lowest errors in specific humidity at lower levels (below ~ 600 hPa), while SAPHIR performs best at higher altitudes. The difference between the super instrument and AMSR-2 demonstrates the additional information SAPHIR provides over AMSR-2 alone.

When interpreting our 1D-Var results we can assess the amount of information extracted from the observations as the degrees of freedom for signal (DFS, see e.g. Rodgers, 2000). We define the averaging kernel matrix \mathbf{V} as

$$\mathbf{V} = \mathbf{I} - \mathbf{AB}^{-1}, \quad (1)$$

where \mathbf{A} and \mathbf{B} are respectively the error covariance matrices for the analysis (retrieved state) and background (initial state). \mathbf{I} is the identity matrix. The DFS is then the trace of the averaging kernel matrix:

$$\text{DFS} = \text{tr}(\mathbf{V}). \quad (2)$$

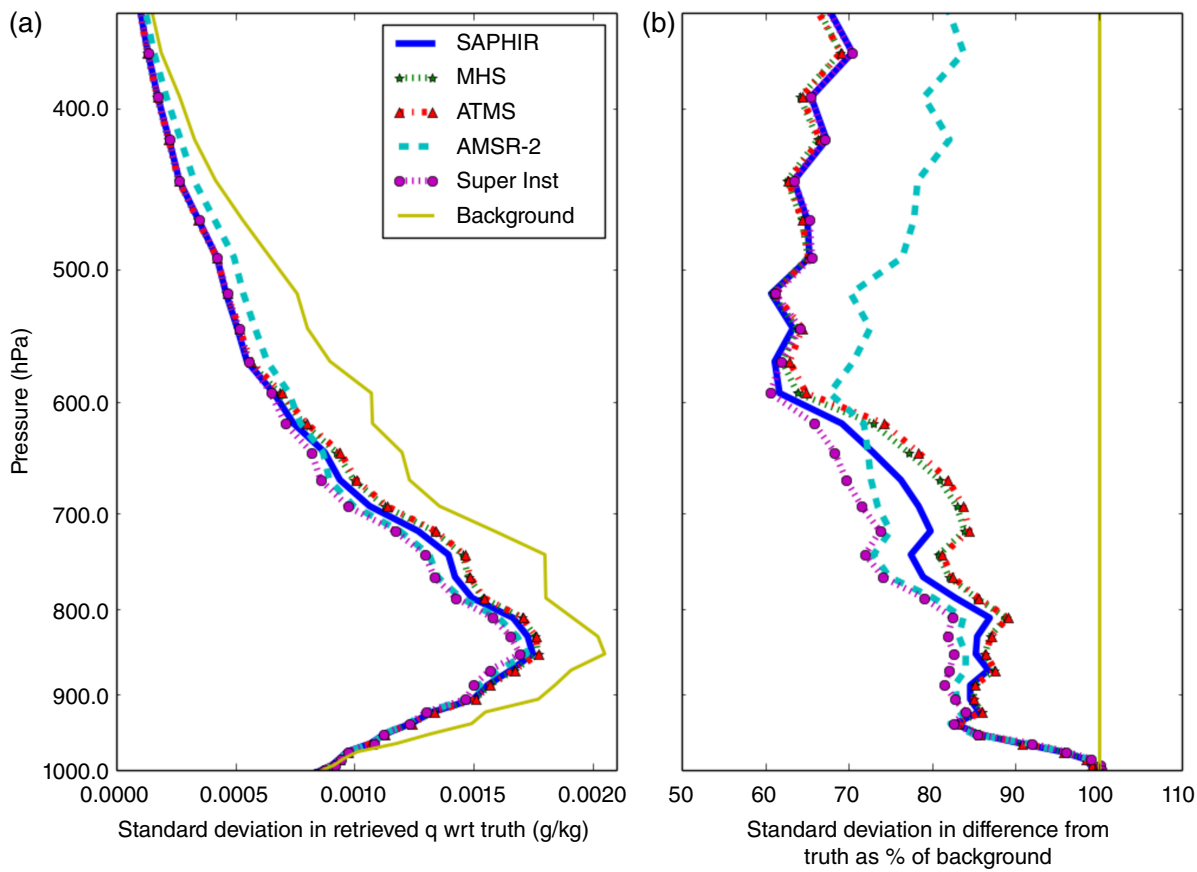


FIGURE 2 Errors (retrieved–true) in the specific humidity profile for each experiment for 1,333 tropical points over ocean shown for each instrument and background as (a) standard deviation in the difference (g/kg), (b) standard deviation as percentage of background standard deviation [Colour figure can be viewed at wileyonlinelibrary.com]

Taking the average over the set of 1,333 1D-Var retrievals, DFS values for the instruments considered (AMSR-2, ATMS, MHS, SAPHIR and the super instrument) are derived as 1.68, 1.50, 1.58, 1.87 and 3.00 respectively. This serves to illustrate both the benefit of extracting information from the suite of six SAPHIR channels compared with the other satellite instruments and the enhanced information content when exploiting the combined channel set of AMSR-2 and SAPHIR.

4 | SINGLE-OBSERVATION EXPERIMENTS

The effect of assimilating single (real) observations on humidity increments using the Met Office data assimilation system can reveal the way in which different instruments and channels affect the humidity analysis. The specific aim here was to investigate how the assimilation of SAPHIR observations altered the increments generated by other observations.

In these experiments, all other satellite data were removed and a single co-located observation from SAPHIR, ATMS and AMSR-2 was assimilated individually, plus an additional experiment assimilating the single observations from the three instruments together. The analysis increments at the location of the observations were examined to give further information about the effect on humidity of each of the instruments alone and all instruments combined.

All SAPHIR and ATMS observations used in the 0000 UTC run of the global forecast on 5 July 2015 were examined. Using trial and error to obtain a reasonable number of matches, spatial/temporal co-location criteria of 2 km and 17 min were selected yielding 22 pairs of co-located observations. These pairs were in turn co-located with AMSR-2 observations from the same period and five points were selected within 7 km and 54 min of the SAPHIR observations (spatial and temporal criteria again selected by trial and error to be the smallest possible while still yielding a non-zero number of matches). Analysis increments were generated by assimilating the single observation from each instrument alone and for all three together at each of these points. Three cases are shown here, selected from the set of five co-locations as being sufficiently different from each other to be of interest. The latitudes and longitudes of the SAPHIR observations are listed in Table 4 with the distance and time between each pair of co-located SAPHIR and AMSR-2 observations. The analysis increment extracted from the assimilation system was also co-located with this position. The ATMS humidity sounding channels were used in the experiment (channels 18–22, Table 1), all SAPHIR channels were used and AMSR-2 channels 7–12 were used following the operational channel selection at the Met Office (Table 3).

Figure 3 shows the vertical profiles of the analysis increments in specific humidity from the surface up to

TABLE 4 The time, latitude and longitude of the positions of the SAPHIR observations on 5 July 2015 and the distance and time difference between the co-located SAPHIR and AMSR-2 observations. These latitudes and longitudes are also the position of the analysis increment from the global output file

Time of SAPHIR ob (UTC)	Latitude (°)	Longitude (°)	Distance between SAPHIR and AMSR-2 ob (km)	Time difference between SAPHIR and AMSR-2 ob (min)
2306	-7.94	40.54	6.2	50
2357	9.14	-152.40	3.8	51.8
2358	9.16	-152.32	0.0	51.8

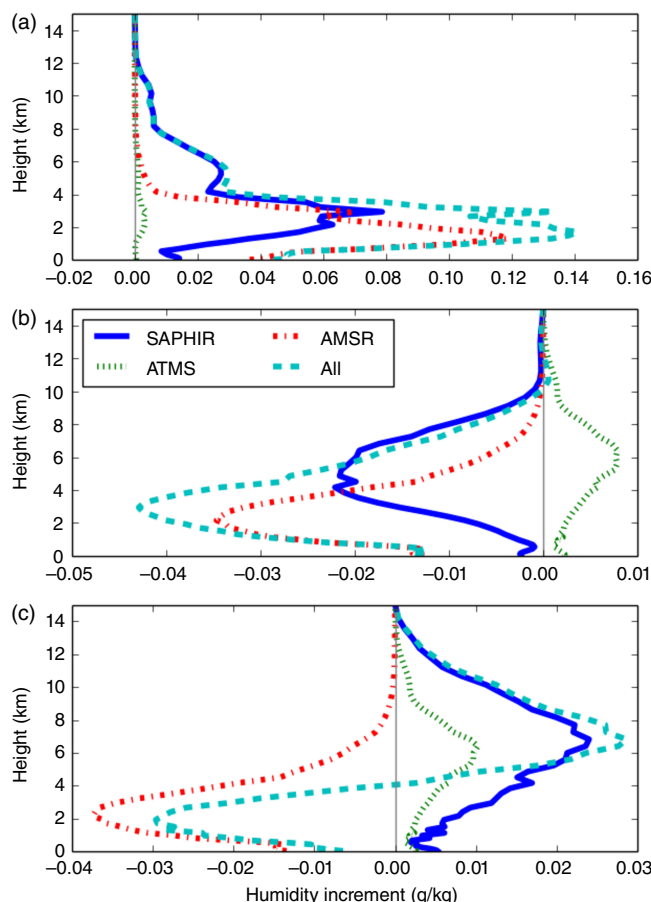


FIGURE 3 Specific humidity analysis increments (g/kg) from the assimilation of a single observation of ATMS, SAPHIR and AMSR-2 alone and all three instruments together at (a) 7.94°S, 40.54°E, (b) 9.14°N, 152.40°W, and (c) 9.16°N 152.32°W between 11 p.m. on 4 July 2015 and 1:00 a.m. on 5 July 2015 [Colour figure can be viewed at wileyonlinelibrary.com]

model level 70, an altitude of approximately 80 km, when SAPHIR, ATMS and AMSR-2 are assimilated individually and when all the three co-located observations are assimilated together.

There are a number of interesting features in Figure 3:

- 1 ATMS, despite having a similar set of channels to SAPHIR, has a much smaller impact on the humidity analysis increments. This is expected to some extent because of the higher observation errors used for ATMS (discussed in

section 2), which will reduce the impact of this instrument. The lower horizontal resolution due to the remapping of the ATMS observations during pre-processing results in a smoothed humidity field, which may reduce the information available from ATMS compared to SAPHIR. AMSR-2 has a large impact on the column total humidity but shows less vertical structure than SAPHIR. The impact of adding SAPHIR is to modify the gross impact of AMSR-2 and add detail to the increments.

- 2 The contribution to analysis increments peaks higher for SAPHIR (usually around 3–6 km) than for AMSR-2 (~1.5–2.0 km). From the weighting function in Figure 1, a modification near the surface might also be expected, but this is not seen here. This is likely due to a greater water vapour burden in the atmosphere at the time of the single-observation experiment which would increase the altitude of the channel 6 SAPHIR weighting function.
- 3 For Figure 3c the sign of the increment is opposite for SAPHIR and AMSR-2 individually, with SAPHIR having a moistening effect and AMSR-2 having a drying effect. This, combined with the different heights of maximum influence for each instrument, results in the combined effect of drying at lower levels and moistening higher in the atmosphere.
- 4 In Figure 3b ATMS increments are in the opposite direction to both SAPHIR and AMSR-2. The time difference in the co-location is particularly large between ATMS and SAPHIR for this point (54 min), so it is possible that a change in conditions occurs between the times of the two observations. Geostationary images from Multifunctional Transport Satellite (MTSAT-2) were examined to support this hypothesis, but resolution of the images is not high enough for confirmation (not shown).

5 | ASSIMILATION EXPERIMENTS

The operational Met Office data assimilation system is based on incremental 4D-Var (Courtier *et al.*, 1994; Rawlins *et al.*, 2007). Data from a range of conventional observations, including surface-based observations, radiosondes, and aircraft-based observations as well as data from satellite instruments are assimilated. This includes five Advanced TIROS Operational Vertical Sounders (ATOVS), (from NOAA-15, NOAA-18, NOAA-19, Metop-A and Metop-B), the Advanced Technology Microwave Sounder (ATMS), advanced infrared sounder data from the Atmospheric Infrared Sounder (AIRS) and the Infrared Atmospheric Sounding Interferometer (IASI), Global Positioning System (GPS) Radio Occultation (GPSRO) data, ground-based GPS, atmospheric motion vectors, geostationary radiances, and scatterometer data.

The Met Office has recently introduced variational bias correction (VarBC) in its deterministic model (Cameron and

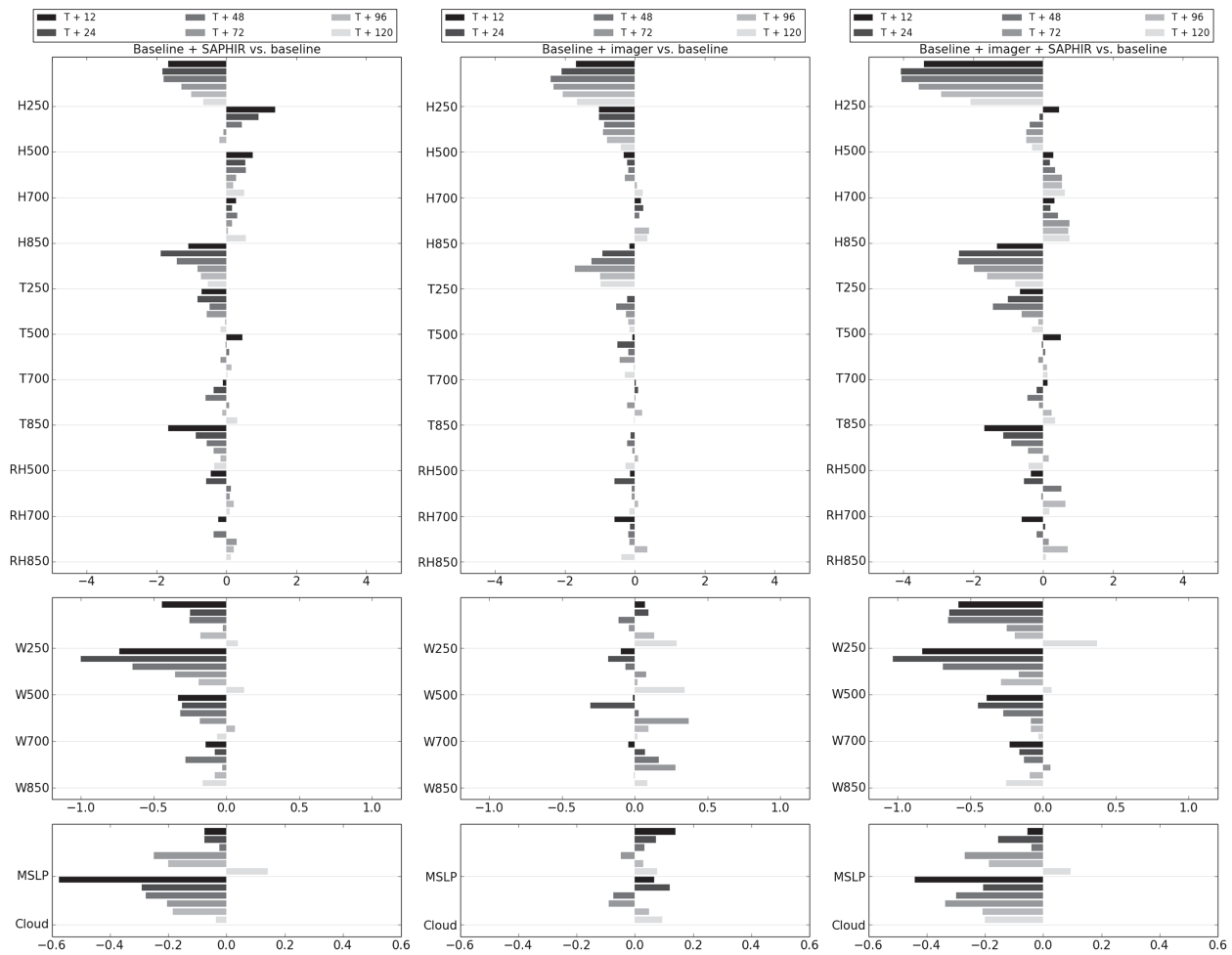


FIGURE 4 A summary of the impacts of the addition of SAPHIR sounding data and microwave imager data to an otherwise full baseline configuration. Verification (percentage change in forecast–observation root-mean-square error) covers the Tropics only (20°N to 20°S), and is relative to the baseline. The experiments were verified for 277 0000 UTC and 1200 UTC forecasts over the period 12 November 2015 to 29 May 2016. Labels for each parameter correspond to geopotential height (“H”), temperature (“T”), relative humidity (“RH”), vector wind (“W”), mean-sea-level pressure (“MSLP”) and cloud amount verified against ceilometer data (“Cloud”). Level-specific parameters are labelled according to pressure in hPa, e.g. “T500” is temperature verified at 500 hPa

Bell, 2015) which is used in the following experiments with a low resolution (N320) version of the Met Office forecast model (horizontal resolution of 0.6° longitude and 0.4° latitude with 70 vertical levels).

The experiments covered the period 5 November 2015 to 29 May 2016. An initial period of 7 days was discarded from the verification to allow for the spin-up of VarBC coefficients. The experiments were then verified for 138 0000 UTC and 139 1200 UTC forecasts, giving a total of 277 forecasts. Experiments were verified relative to a baseline configuration, or control, which comprised the full Met Office observing system minus the microwave imagers (AMSR-2 and SSMIS) and SAPHIR. SAPHIR and the imagers were added separately and together, giving a total of four assimilation experiments (one control and three tests). The results are summarised in Figure 4.

From Figure 4 it can be seen that SAPHIR alone has a positive impact at the 12–48 h forecast lead time on temperature at 250 and 500 hPa and on relative humidity at 500 hPa with a 1–2% improvement in root-mean-square error (RMSE) seen in these parameters. For wind speed and direction the addition

of SAPHIR reduces RMSE at these shorter forecast times by 0.5–1% at 850–100 hPa. When the imagers (Special Sensor Microwave Imager/Sounder (SSMIS) imaging channels plus AMSR-2) are added to the baseline system, the impact on temperature and relative humidity RMSE is smaller compared to that seen from SAPHIR, although still positive, but for the wind speed a degradation is seen when imaging channels are added. The right-hand column in Figure 4 shows the impact on RMSE when SAPHIR and the imagers are assimilated together. Impact is improved in almost all cases, notably temperature at 250 hPa shows a decrease in RMSE of ~2% for all forecast lead times. In the case of the RMSE for the wind vectors the combined SAPHIR+imagers impact shows all of the positive benefit of the individual experiments and none of the degradation, improving the RMSE of wind at 500 hPa T + 24 h forecast by more than 1%.

The impact of a change to the assimilation system can also be assessed by looking at the change in standard deviation of the background fit to other sounding observations. Figure 5 shows the percentage change in standard deviation for IASI, AIRS and Cross-track Infrared Sounder (CrIS) when SAPHIR

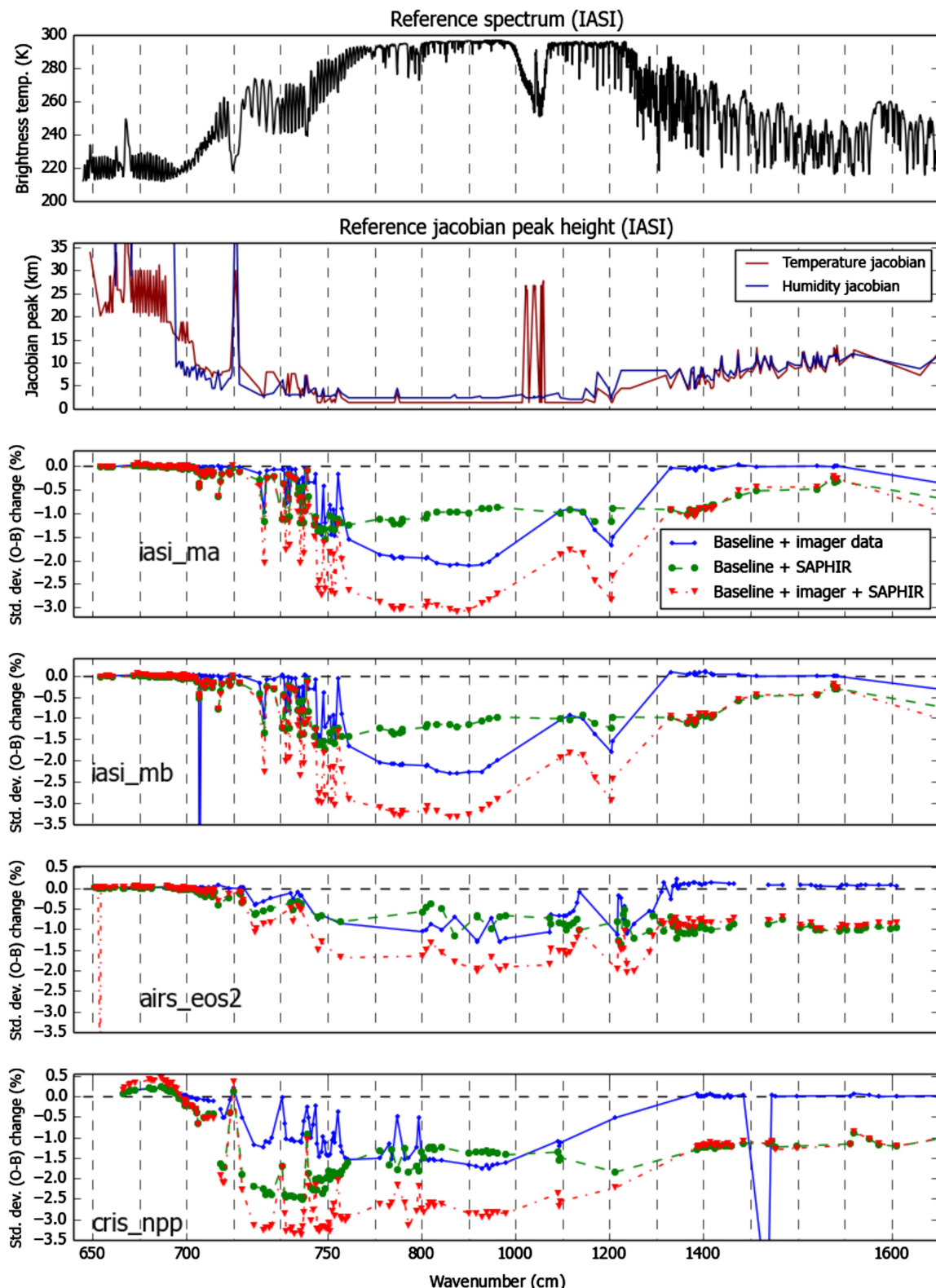


FIGURE 5 Percentage changes in (STDEV) of background fits to IASI, AIRS and CrIS in the Met Office NWP system for a 6-month trial on top of an otherwise complete baseline, when SAPHIR and AMSR-2 are assimilated separately and together [Colour figure can be viewed at wileyonlinelibrary.com]

and AMSR-2 are added alone and together; Figure 6 shows the same information for each of the AMSU-A instruments and ATMS temperature sounding channels and Figure 7 for AMSU-B/MHS and the humidity sounding channels on ATMS. For the advanced IR sounders in Figure 5, improvements are seen in all cases, with the improvement when both

SAPHIR and AMSR-2 are assimilated significantly larger than for either instrument alone. Figure 6 shows more mixed and smaller impact; in general, improvement is seen but occasionally there is some small degradation (e.g. ATMS channels 6 and 7). The difference between assimilating both instruments and either one alone is less pronounced. For MHS

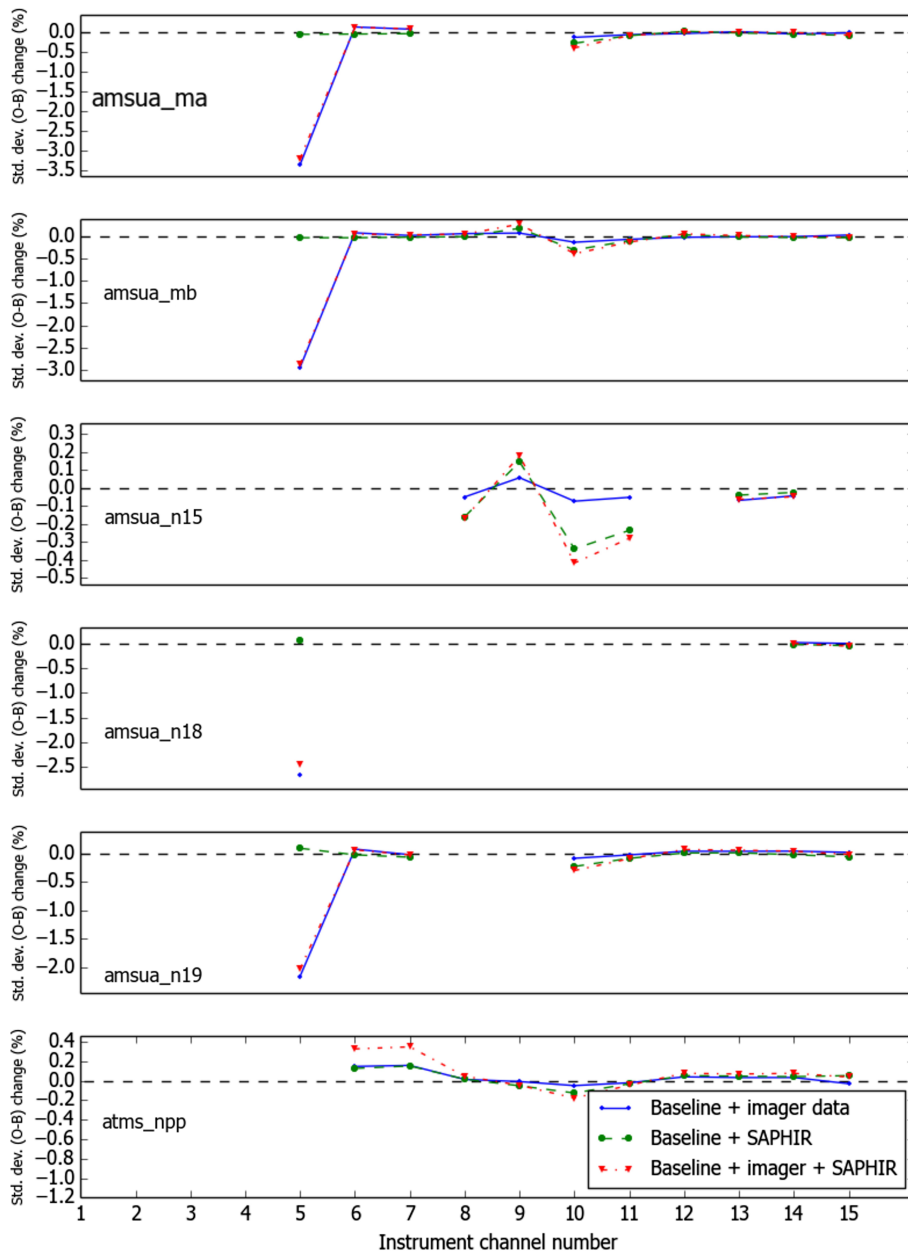


FIGURE 6 As Figure 5, for AMSU-A and ATMS temperature sounding channels [Colour figure can be viewed at wileyonlinelibrary.com]

and MHS-like channels in Figure 7, adding either instrument alone gives a decrease in standard deviation, with SAPHIR having by far the larger effect. This is expected as the SAPHIR channels are at similar frequencies to these. The improvement when adding both instruments together is not significant for these instruments.

6 | SPIN-DOWN

Previous investigations into the impact of the assimilation of microwave imager observations at the Met Office have frequently highlighted a problem with the spin-down of precipitation in the forecast model, particularly in the Tropics. We speculate that this is caused by the relative lack of observational information in constraining the vertical

structure of the humidity increments, which is controlled largely by the form of the assumed background error correlations. The humidity increments are then often not in balance with the representation of moist processes in the nonlinear forecast model. The consequence of this is that the forecast model precipitation fields show anomalously large values in the early period of the forecast, which then subsequently relax (“spin down”) at longer forecast ranges.

In order to test the hypothesis that the assimilation of the SAPHIR data in conjunction with the microwave imager data (from AMSR-2) results in more accurate humidity increments which should be in better balance with the model’s moist physics, the evolution of precipitation in the Tropics was inspected for experiments in which either or both, or none, of the SAPHIR and AMSR-2 data was assimilated.

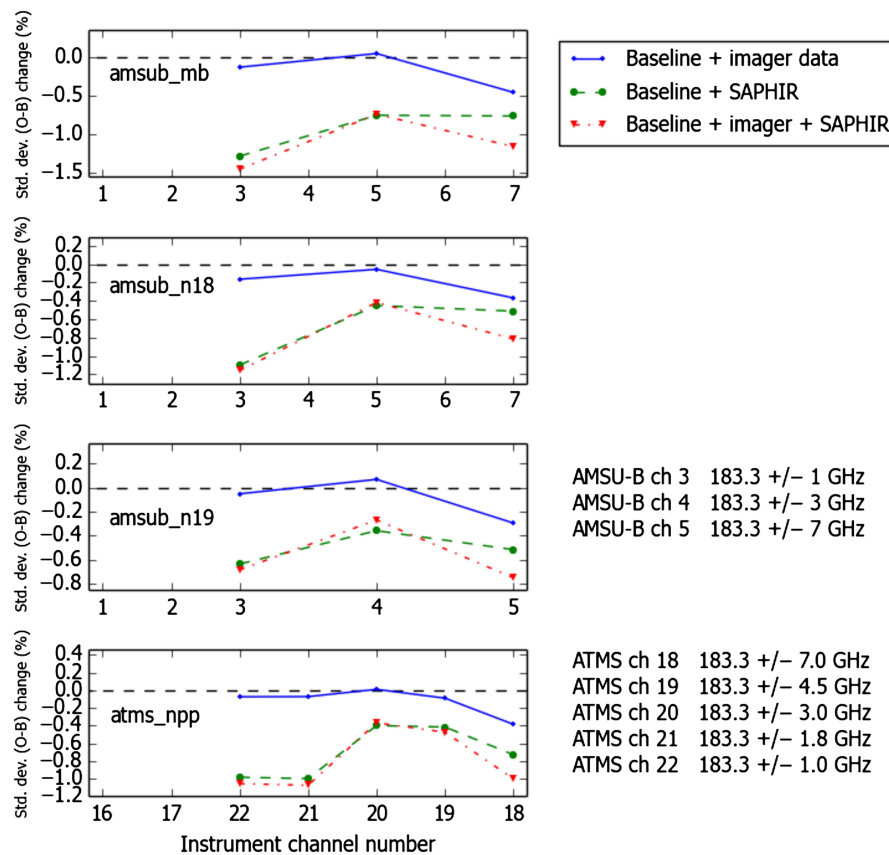


FIGURE 7 As Figure 5, for AMSU-B (MHS) and ATMS humidity sounding channels [Colour figure can be viewed at wileyonlinelibrary.com]

A number of single cycles of the NWP system were run during July and August 2016; the same cycles were run four times with different combinations of observations assimilated:

- 1 Neither SAPHIR nor AMSR-2 assimilated (control)
- 2 SAPHIR assimilated, no AMSR-2
- 3 AMSR-2 assimilated, no SAPHIR
- 4 Both SAPHIR and AMSR-2 assimilated.

Two regions were chosen to investigate the effect of SAPHIR data on the spin-down, one over the Pacific and one over the Indian Ocean. The diurnal cycle of precipitation may have an impact on the spin-down effect so an average was taken of the convective precipitation output every 12 min time step from 19 cycles at each of the normal cycle times of the Met Office forecast (0000, 0600, 1200 and 1800 UTC). These times correspond to local times of 5:00 a.m., 11:00 a.m., 5:00 p.m. and 11:00 p.m. for the Indian Ocean region and 11 and 12 h ahead for the Pacific Ocean region which spans two time zones (11:00 a.m. to 12 noon, 5:00 p.m. to 6:00 p.m., 11:00 p.m. to midnight, 5:00 a.m. to 6:00 a.m.). The diurnal cycle of precipitation over ocean in the Tropics is not as pronounced as that over land, but generally shows maxima in late-evening–early-morning local time (Nesbitt and Zipser, 2003; Yang and Smith, 2006).

Examples of the convective rain rate as it evolves over the period of the forecast are shown in Figure 8. Figure 8a,b are for the Pacific and Indian Ocean regions respectively for the 0000 UTC cycle (11:00 a.m. and 5:00 a.m. local time)

and clearly show that SAPHIR + AMSR-2 data reduces the spin-down effect by minimising the shock in the first time step and resulting in a forecast rain rate lower than for either instrument alone. This reduction is roughly $0.5 \times 10^{-4} \text{ kg m}^{-2} \text{ s}^{-1}$ for the Pacific region and $0.1 \text{ kg m}^{-2} \text{ s}^{-1}$ for the Indian Ocean region. Figure 8c,d show the same as Figure 8a,b, but for the 1800 UTC cycle (11:00 p.m. and 5:00 a.m. local time); here the impact of SAPHIR is less distinct, although the initial spin-down effect itself is also not as pronounced. For the Pacific region (Figure 8c) there is no spin-down to be seen in the control, and SAPHIR has a drying effect at all time steps. For the Indian Ocean region (Figure 8d) the spin-down effect is exaggerated by the introduction of AMSR-2 and this is then modified when SAPHIR is also added, although the effect is still amplified compared to control. Interestingly the effect of SAPHIR alone added to the control in this case gives the lowest rain rate increase of the three experiments.

7 | CONCLUSIONS

SAPHIR offers improved humidity sounding in the Tropics, with higher vertical, horizontal and temporal resolution than current similar microwave humidity sounders. This article examined how these improvements translate into improvements in analyses and forecasts when SAPHIR data is assimilated within a global NWP system.

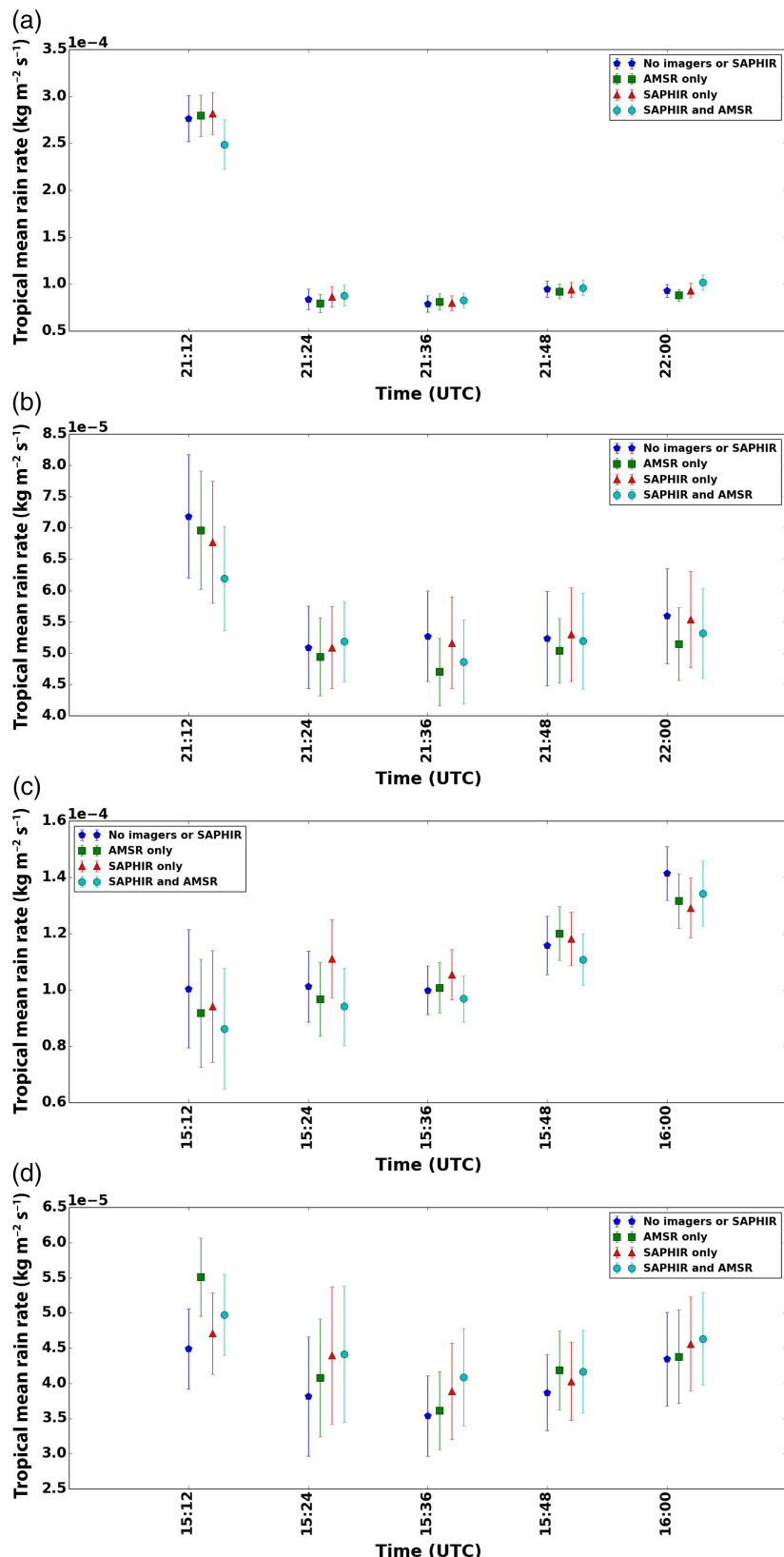


FIGURE 8 Forecast rain rate per time step, mean of 19 forecast cycles at the same time of day, for control and three experiments for (a) the 0000 UTC run over the Pacific Ocean, (b) the 0000 UTC run over the Indian Ocean, (c) the 1800 UTC run over the Pacific, and (d) the 1800 UTC run over the Indian Ocean [Colour figure can be viewed at wileyonlinelibrary.com]

Initial idealized 1D-Var experiments showed that SAPHIR allows a more accurate retrieval of humidity than similar satellite humidity sounders (MHS, ATMS). When used together with AMSR-2 the retrieval is improved at higher

altitudes (above ~ 600 hPa) over the use of AMSR-2 alone. An inspection of humidity analysis increments from single-observation experiments in the Met Office NWP system confirmed that a single SAPHIR observation has

a beneficial impact on the representation of moisture within the model. This impact is enhanced when SAPHIR is added together with AMSR-2, with SAPHIR adding vertical detail to the humidity information provided by AMSR-2.

Assimilation experiments adding SAPHIR and AMSR-2 to a low-resolution version of the full Met Office NWP system improved the NWP forecast performance; for example, RMSE of temperature and relative humidity forecasts at 500 hPa were improved by 1–2%. Background fits to other observations with sensitivity to humidity were improved: window channels for hyperspectral IR sounders (AIRS, IASI, CrIS) showed ~1% reductions in standard deviation of first guess departures. These improvements were greater than when either SAPHIR or AMSR-2 were added alone, confirming the complementarity between the two instruments. For example, upper-level winds (at 100 and 250 hPa) were improved by approximately 0.5% for Day 1 to Day 3 forecasts when SAPHIR and AMSR-2 were added together, whereas less positive benefits were observed when SAPHIR or AMSR-2 were added individually.

Finally, it was observed that the assimilation of SAPHIR and AMSR-2 data reduced anomalously large precipitation rates in the Tropics in the first time steps of the forecast model, suggesting the analysis generated by the assimilation of these data is in better balance with the representation of moist physics in the forecast model.

The results reported here demonstrate that SAPHIR's unique new capabilities deliver measurable benefits in the Met Office operational global model. The results support consideration of the enhanced SAPHIR channel set, and low inclination orbit, for future operational missions. The complementarity between SAPHIR and AMSR-2 in providing improved humidity information is clear, validating the "proof of concept" of the intended payload for MT which included MADRAS. MADRAS has similar channels to AMSR-2, which flying on the same platform as SAPHIR would have been of great benefit in NWP. Looking to the future the authors note that the MetOp-SG payload due for first launch in the early 2020s does not include SAPHIR-like channels. The Ice Cloud Imager (ICI) has three channels centred on the 183 GHz line, at ±8.4, ±3.4 and ±2, while the Microwave Sounder (MWS) will replicate the five ATMS channel frequencies near 183 GHz. Based on the outcomes of this study we would contend that the higher peaking of the SAPHIR channels (±0.2) adds significant benefit in NWP, and we regret that such a channel has not been included on the MetOp-SG missions.

ACKNOWLEDGEMENTS

We thank Stephan Havemann for useful discussions on 1D-Var retrieval information content and Crispian Batstone for help with retrieving the MTSAT-2 images from the Met Office Tigger database. Thanks also to the anonymous

reviewers whose comments have helped to improve the article.

The authors would also like to acknowledge the funding for visiting scientists missions without which the work of this article would not have been possible, the first from September 2014 to March 2015 funded by the Indian National Monsoon Mission, Ministry of Earth Sciences, Government of India, the second in July 2016, funded by the NWPSAF Visiting Scientist Program.

REFERENCES

- Bennartz, R., Thoss, A., Dybbroe, A. and Michelson, D.B. (2002) Precipitation analysis using the advanced microwave sounding unit in support of nowcasting applications. *Meteorological Applications*, 9, 177–189.
- Brogniez, H., English, S., Mahfouf, J.-F., Behrendt, A., Berg, W., Boukabara, S., Buehler, S.A., Chambon, P., Gambacorta, A., Geer, A., Ingram, W., Kursinski, E.R., Matricardi, M., Odintsova, T.A., Payne, V., Thorne, P.W., Tretyakov, M.Y. and Wang, J. (2016) A review of sources of systematic errors and uncertainties in observations and simulations at 183 GHz. *Atmospheric Measurement Techniques*, 9, 2207–2221. <https://doi.org/10.5194/amt-9-2207-2016>.
- Brogniez, H., Kirstetter, P.-E. and Eymard, L. (2013) Expected improvements in the atmospheric humidity profile retrieval using the Megha-Tropiques microwave payload. *Quarterly Journal of the Royal Meteorological Society*, 139, 842–851.
- Cameron, J. and Bell, W. (2015) *Pre-operational testing of variational bias correction (VarBC)*. Satellite Applications Technical Memo. 37. Exeter, UK: Met Office.
- Chambon, P., Meunier, L.-F., Guillaume, F., Piriou, J.-M., Roca, R. and Mahfouf, J.-F. (2015) Investigating the impact of the water-vapour sounding observations from SAPHIR on board Megha-Tropiques for the ARPEGE global model. *Quarterly Journal of the Royal Meteorological Society*, 141, 1769–1779.
- Chevalier, F. (2001) *Sampled databases of 60-level atmospheric profiles from the ECMWF analyses*. EUMETSAT/ECMWF SAF programme research report no. 4. Available at: http://nwpsaf.eu/downloads/profiles/profiles_60L.pdf
- Clain, G., Brogniez, H., Payne, V.H., John, V.O. and Luo, M. (2015) An assessment of SAPHIR calibration using quality tropical soundings. *Journal of Atmospheric and Oceanic Technology*, 32, 61–78. <https://doi.org/10.1175/JTECH-D-14-00054.1>.
- Courtier, P., Thépaut, J.-N. and Hollingsworth, A. (1994) A strategy for operational implementation of 4D-Var, using an incremental approach. *Quarterly Journal of the Royal Meteorological Society*, 120, 1367–1387.
- Doherty, A.M., Atkinson, N., Bell, W., Candy, B., Keogh, S. and Cooper, C. (2012) *An initial assessment of data from the advanced technology microwave sounder*. Met Office Technical Report 569. Exeter, UK. Available at: <https://digital.nmla.metoffice.gov.uk/file/sdb%3AdigitalFile%7C0b4f64ef-210d-4cd0-a6c8-bbd5039984ee/>
- Doherty, A.M., Atkinson, N., Bell, W. and Smith, A. (2015) An assessment of data from the Advanced Technology Microwave Sounder at the Met Office. *Advances in Meteorology*, 2015, 16. <https://doi.org/10.1155/2015/956920>.
- Fisher, M. and Courtier, P. (1995) *Estimating the covariance matrices of analysis and forecast error in variational data assimilation*. ECMWF Technical Memorandum 220, Shinfield Park, Reading, UK. Available at: <http://www.ecmwf.int/publications/>
- Labrot, T., Lavanant, L., Whyte, K., Atkinson, N. and Brunel, P. (2006) *AAPP documentation, scientific description*. NWP SAF Document NWPSAF-MF-UD-001. Exeter, UK.
- Moradi, I. (2014) Inter-calibration of observations from SAPHIR and ATMS instruments. *GSICS Quarterly*, 8. <https://doi.org/10.7289/V55H7D64>.
- Nesbitt, S.W. and Zipser, E.J. (2003) The diurnal cycle of rainfall and convective intensity according to three years of TRMM measurements. *Journal of Climate*, 16, 1456–1475. <https://doi.org/10.1175/1520-0442-16.10.1456>.
- Numerical Weather Prediction Satellite Application Facility. (2011) *Annex to AAPP scientific documentation: pre-processing of ATMS and CrIS*. Document NWPSAF-MO-UD-027. Exeter, UK. Available at: http://nwpsaf.eu/deliverables/aapp/NWPSAF-MO-UD-027_ATMS_CrIS.pdf
- Rani, I., Bell, W., Doherty, A.M. and Newman, S. (2016) *An investigation of the impact of the assimilation of M-T SAPHIR data in the Met Office data*

- assimilation system. NWPSAF report of visiting scientist mission NWP_VS16_03. Exeter, UK. Document NWPSAF-MO-VS-055. Available at: https://nwpsaf.eu/vs_reports/nwpsaf-mo-vs-055.pdf
- Rawlins, F., Ballard, S.P., Bovis, K.J., Clayton, A.M., Li, D., Inverarity, G.W., Lorenc, A.C., Buehler, S.A., Chambon, P., Gambacorta, A., Geer, A., Ingram, W., Kursinski, E.R., Matricardi, M., Odintsova, T.A., Payne, V., Thorne, P.W., Tretyakov, M.Y. and Payne, T.J. (2007) The Met Office global four-dimensional variational data assimilation scheme. *Quarterly Journal of the Royal Meteorological Society*, 133, 347–362.
- Roca, R., Brogniez, H., Chambon, P., Chomette, O., Cloche, S., Gosset, M.E., Mahfouf, J.-F., Raberanto, P. and Viltard, N. (2015) The Megha-Tropiques mission: a review after three years in orbit. *Frontiers in Earth Science*, 3, 17. <https://doi.org/10.3389/feart.2015.00017>.
- Rodgers, C.D. (2000) *Inverse Methods for Atmospheric Sounding: Theory and Practice*. Singapore: World Scientific.
- Saunders, R. (2010) *RTTOV9 science and validation report*. Document NWPSAF-MO-TV-020. Exeter, UK. Available at: http://nwpsaf.eu/oldsite/deliverables/rtm/rttov9_files/rttov9_svr.pdf
- Saunders, R., Hocking, J., Rundle, D., Rayer, P., Havemann, S., Matricardi, M., Geer, A., Lupu, C., Brunel, P. and Vidot, J. (2017) *RTTOV12 science and validation report*. Document NWPSAF-MO-TV-41. Exeter, UK. Available at: http://nwpsaf.eu/deliverables/rtm/docs_rttov12/rttov12_svr.pdf
- Singh, R., Ojha, S.P., Kishtawal, C.M. and Pal, P.K. (2013) Quality assessment and assimilation of Megha-Tropiques SAPHIR radiances into WRF assimilation system. *Journal of Geophysical Research: Atmospheres*, 118, 6957–6969. <https://doi.org/10.1002/jgrd.50502>.
- Smith, F. (2016) *NWPSAF 1D-Var user manual software version 1.1*. Exeter, UK. Available at: https://nwpsaf.eu/site/download/documentation/1dvar/nwpsaf-mo-ud-032_NWPSAF_1DVar_Manual.pdf
- Vijayasree, P., Kumar, N., Karidhal, R., Harendranath, K., Raju, V.K. and Shivakumar, S.K. (2014) Megha-Tropiques: mission planning, analysis, and operations. *International Journal of Remote Sensing*, 35, 5370–5383. Special Issue: SI. <https://doi.org/10.1080/01431161.2014.926412>.
- World Meteorological Organisation. (2017) *Observing System Capability Analysis and Review tool (OSCAR) database*. Geneva, Switzerland. Available at: <https://www.wmo-sat.info/oscar/>
- Yang, S. and Smith, E.A. (2006) Mechanisms for diurnal variability of global tropical rainfall observed from TRMM. *Journal of Climate*, 19, 5190–5226. <https://doi.org/10.1175/JCLI3883.1>.

How to cite this article: Doherty A, Indira Rani S, Newman S, Bell W. Benefits of assimilating SAPHIR observations on analysis and forecasts of tropical fields in the Met Office global model. *Q J R Meteorol Soc* 2018;1–14. <https://doi.org/10.1002/qj.3258>